STATISTICS, OPTIMIZATION AND INFORMATION COMPUTING
Stat., Optim. Inf. Comput., Vol. **12**, March 2024, pp 463–487.
Published online in International Academic Press (www.IAPress.org)

Risk Assessment in Cryptocurrency Portfolios: a Composite Hidden Markov Factor Analysis Framework

Mohamed Saidane*

Department of Management Information Systems and Production Management, College of Business and Economics, Qassim University, kingdom of Saudi Arabia

Abstract In this paper, we deal with the estimation of two widely used risk measures such as Value-at-Risk (VaR) and Expected Shortfall (ES) in a cryptocurrency context. To face the presence of regime switching in the cryptocurrency volatilities and the dynamic interconnection between them, we propose a Monte Carlo-based approach using heteroskedastic factor analysis and hidden Markov models (HMM) combined with a structured variational Expectation-Maximization (EM) learning approach. This composite approach allows the construction of a diversified portfolio and determines an optimal allocation strategy making it possible to minimize the conditional risk of the portfolio and maximize the return. The out-of-sample prediction experiments show that the composite factorial HMM approach performs better, in terms of prediction accuracy, than some other baseline methods presented in the literature. Moreover, our results show that the proposed methodology provides the best performing crypto-asset allocation strategies and it is also clearly superior to the existing methods in VaR and ES predictions.

Keywords Factor analysis, HMM, Variational-EM, Dynamic forecasting, Crypto asset allocation, VaR - ES

AMS 2010 subject classifications 62H25, 62M05, 62M10, 62M20, 62P05

DOI: 10.19139/soic-2310-5070-1837

1. Introduction

Crypto (digital, virtual) currencies have experienced a spectacular boom over the past decade. In the first six months of 2021, the number of cryptocurrency users worldwide doubled to 221 million, including 114 million Bitcoin and 23 million Ethereum holders. As for the total cryptocurrency market capitalization, it has multiplied by ten in less than two years, to exceed 2.6 trillion dollars in November 2021. After a sharp decline by nearly 1,500 billion dollars on January 2022, the market then rose by nearly 2,000 billion at the beginning of April.[†] The Bitcoin (more than 800 billion in capitalization) and the Ethereum (nearly 400 billion), together hold two-thirds of the market. According to the Financial Stability Board, the supervisor of global finance, cryptocurrencies today represent 1% of global financial assets.

From a practical point of view, the main advantages of cryptocurrency are instantaneous and secure transactions; they are carried out without the intermediary of a bank. Many web services and merchants have chosen to accept it as a method of payment, attracted by the absence of transaction fees and the irrevocable nature of validated transactions.

Cryptocurrencies have become, since 2017, a financial asset in their own right. A highly speculative asset, whose price is subject to wide variations, both up and down. With prospects of record gains for investors, but also high

*Correspondence to: Mohamed Saidane (Email: M.Saidane@qu.edu.sa). Department of Management Information Systems and Production Management, College of Business and Economics, Qassim University. P.O. Box 6666 - Buraidah, kingdom of Saudi Arabia (51452).
[†]See e.g. https://coinmarketcap.com/charts/.

ISSN 2310-5070 (online) ISSN 2311-004X (print)

risks of capital loss. This market is indeed particularly volatile, marked by strong and unexpected depreciations, over very short periods, like the brutal collapse, at the beginning of the year, of the value of Bitcoin, which went from more than 69,000 USD in November 2021 to 36,000 USD on January 2022, before rising to 42,500 USD on April 2022, then starting a new decline. Hence, there is a need to predict and control the risks associated with cryptocurrencies. To do this, we find that the traditional historical simulation approach, or GARCH-type methods are too restrictive. More general Markov-switching multivariate methods provide more flexibility to account for such non-standard time series behavior that might be attributed to a large extend to speculators.

We propose in this paper a new composite hidden Markov factor analysis approach for crypto-portfolios risk prediction, using Value-at-Risk (VaR) and expected shortfall (ES) as risk measurements. Our multivariate sequential forecasting strategy allows for time-varying volatility as well as the possibility of regime switching in the crypto asset prices. A structured variational expectation maximization (EM) algorithm for the inference of the latent structures and the updating of the model's parameters is also proposed.

Markov switching models with time-varying volatility have showed an outstanding performance than have standard models in the presence of volatility shifts (see Trucios, 2019; Troster et al., 2019 and Charles and Darné, 2019). Furthermore, when used to model the dependance structures of multiple asset classes, latent factor analysis models have been shown to perform better than copula models (Yu et al., 2018 and Abbara and Zevallos, 2018). In such a setting, a Monte-Calo-based composite hidden Markov factor analysis approach for VaR and ES predictions could be interesting for investors.

This paper contributes to the growing literature on crypto asset allocation and portfolio risk measurement. The most discussed approaches in the previous literature include ARMA-GARCH models (Platanakis and Urquhart, 2019) as well as the generalized autoregressive score models used by Liu et al., (2020), extreme value theory models used by Gkillas and Katsiampa (2018), copula-based modeling approaches (e.g., Trucios et al., 2020), GARCH models with Markov-Switching dynamics used by Maciel, (2020), dynamic latent factor analysis models used by Saidane and Lavergne (2009, 2011) and Saidane (2022a,b, 2023) and some prediction methods using machine learning techniques like those employed by Takeda and Sugiyama (2008). The previous literature contains also empirical studies on portfolio diversification strategies using a mix of traditional and crypto assets (e.g., Petukhina et al., 2021 and Elendner et al., 2017). This evokes once again the interest of finding more flexible new sequential allocation strategies to predict and analyse cryptocurrency portfolios risk. In this context, our contribution comes through the development of a model that takes into account both the time-varying correlations between crypto assets, as well as, the regime-switching behavior of the portfolio volatility, an approach never used previously in the risk assessment of crypto-portfolios.

The remaining of this paper is structured as follows. In section 2, we present the theoretical description of the composite hidden Markov factor analysis model. Then, we present our Variational-EM approach to infer the latent state variables and estimate the model's parameters. The dynamic crypto asset allocation strategies as well as the the Monte Carlo-based VaR and ES prediction methodology will de described in section 3. In section 4, the forecasting performance of our proposed model will be compared with that of other baseline prediction methods presented in the literature. The performance of the VaR and ES measures generated by the different sequential allocation strategies will also be discussed in section 4. Finally, we conclude the article with a brief discussion of the main results and the perspectives for potential future developments.

2. Mathematical formulation of the proposed model

We briefly describe in this section the model used to predict the VaR and ES of the cryptocurrencies' portfolio. Our methodology is based on factor analysis with time-varying volatility combined with hidden Markov models. In section 2.1 we define the Markov-switching dynamic factorial structure and the basic identification and stationnarity assumptions under which the estimation method is developed. The inference procedure of the common latent factors using a switching Kalman filtering algorithm is also described. Thereafter, in section 2.2 we describe the proposed estimation method based on the combination of the EM algorithm (Dempster, et al., 1977) with an approximate variational procedure (Saidane and Lavergne, 2007a).

2.1. Dynamic factor structure

In a matrix notation, the composite hidden Markov factor analysis (CHMFA) framework for the q-vector of crypto asset returns $\mathbf{r}_t$ under the market regime j at time t, is given by:

$$\mathbf{r}_t = \mathbf{B}_j \mathbf{f}_t + \boldsymbol{\epsilon}_t \tag{1}$$

where, $\forall\, t = 1, ..., n_o$, $\forall\, j = 1, ..., n_s$, the k-vector of conditionally heteroskedastic common factors is given by:

$$\mathbf{f}_t \sim \mathcal{N}(\mathbf{0}, \mathbf{H}_{jt}) \tag{2}$$

In this case, $\forall\, l = 1, ..., k$, each latent factor f_{lt} follows a first order generalized quadratic autoregressive conditionally heteroskedastic, GQARCH-type processes (Saidane, 2009). The l-th element of the diagonal covariance matrix $\mathbf{H}_{jt}$, is given by:

$$h^j_{lt} = a_{1jl} + a_{2jl} f^j_{lt-1} + a_{3jl} f^{j\,2}_{lt-1} + a_{4jl} h^j_{lt-1} \tag{3}$$

Hence, the common variances are assumed to be time-varying and their parameters change according to the regime.

Finally, the idiosyncratic factor vectors are given by:

$$\boldsymbol{\epsilon}_t \sim \mathcal{N}(\boldsymbol{\mu}_j, \boldsymbol{\Psi}_j) \tag{4}$$

In this framework the switching between different regimes is governed by a first-order homogeneous Markov process. Specifically, for a given hidden state $S_t = j$, $\boldsymbol{\mu}_j$ is the q-vector of specific means, $\mathbf{B}_j$ the $(q \times k)$ factor loadings matrix, and $\boldsymbol{\Psi}_j$ the $(q \times q)$ diagonal and definite positive matrix of specific or idiosyncratic variances.

We constrain the parameters a_{1jl}, a_{3jl} ,a_{4jl} to be greater than zero to ensure the non-negativity of the conditional common variances as well as $a^2_{2jl} \leq 4 a_{1jl} a_{3jl}$ and $a_{3jl} + a_{4jl} < 1$, $\forall\, j,\, l$ to obtain a stationary covariance process. To ensure the identification of the model, it is required that $q \geq k$ and $rank(\mathbf{B}_j) = k$, $\forall\, j$. Furthermore, we assume non-correlated specific factors and mutual independence between $\mathbf{f}_t$ and $\boldsymbol{\epsilon}_{t'}$ for all $t,\, t'$.

Our model can also be expressed by the following dynamic state-space equations:

$$\mathbf{r}_t = \boldsymbol{\mu}_j + \mathbf{B}_j \mathbf{f}_t + \boldsymbol{\upsilon}_t \tag{5}$$

and

$$\mathbf{f}_t = \mathbf{0} \cdot \mathbf{f}_{t-1} + \mathbf{H}^{\frac{1}{2}}_{jt} \boldsymbol{\nu}_t \tag{6}$$

where $\boldsymbol{\upsilon}_t | \mathcal{D}_{1:t-1} \sim \mathcal{N}(\mathbf{0}, \boldsymbol{\Psi}_j)$ and $\boldsymbol{\nu}_t \sim \mathcal{N}(\mathbf{0}, \mathbf{I}_k)$. The time-$t$ information set is denoted by $\mathcal{D}_{1:t-1} = \{\mathcal{R}_{1:t-1}, \mathcal{F}_{1:t-1}, \mathcal{S}_{1:t-1}\}$, where $\mathcal{R}_{1:\tau} = \{\mathbf{r}_1, ..., \mathbf{r}_\tau\}$, $\mathcal{F}_{1:\tau} = \{\mathbf{f}_1, ..., \mathbf{f}_\tau\}$ and $\mathcal{S}_{1:\tau} = \{S_1, ..., S_\tau\}$. Therefore, from these equations the recursive switching Kalman filter is constructed starting with the following prediction equations:

$$\begin{aligned} \mathbb{E}(\mathbf{f}_{t+1} | \mathcal{D}_{1:t}) &= \mathbf{f}^j_{t+1|t} = \mathbf{0} \cdot \mathbf{f}^j_{t|t} = \mathbf{0} \\ Var(f_{lt+1} | \mathcal{D}_{1:t}) &= h^j_{lt+1|t} = a_{1jl} + a_{2jl} f^j_{lt|t} + a_{3jl} \left[f^{j\,2}_{lt|t} + h^j_{lt|t} \right] + a_{4jl} h^j_{lt|t-1} \end{aligned}$$

where $\forall\, j = 1, ..., n_s$, $f^j_{lt|t} = \mathbb{E}(f^j_{lt} | \mathcal{D}_{1:t})$ and $h^j_{lt|t} = Var(f^j_{lt} | \mathcal{D}_{1:t})$, which represent the elements of the first diagonal of $\mathbf{H}^j_{t|t}$. In this case, the terms $h^j_{lt|t}$ come from the global variance formula as follows:

$$\mathbb{E}(f^{j2}_{lt} | \mathcal{D}_{1:t}) = Var(f^j_{lt} | \mathcal{D}_{1:t}) + \mathbb{E}(f^j_{lt} | \mathcal{D}_{1:t})^2 = h^j_{lt|t} + f^{j2}_{lt|t}$$

Now we can apply a modified version of the Kalman filtering algorithm obtained by generalizing the approach of Saidane and Lavergne (2011) in order to get the best estimates (in the conditional mean square sense) for the common latent factors as follows:

$$\begin{aligned}\mathbf{f}^j_{t+1|t+1} &= \mathbf{H}^j_{t+1|t}\mathbf{B}'_j\left[\mathbf{\Omega}^j_{t+1|t}\right]^{-1}(\mathbf{r}_t-\boldsymbol{\mu}_j)\\ \mathbf{H}^j_{t+1|t+1} &= \mathbf{H}^j_{t+1|t}-\mathbf{H}^j_{t+1|t}\mathbf{B}'_j\left[\mathbf{\Omega}^j_{t+1|t}\right]^{-1}\mathbf{B}_j\mathbf{H}^j_{t+1|t}\end{aligned}$$

where $\mathbf{\Omega}^j_{t+1|t}=\mathbf{B}_j\mathbf{H}^j_{t+1|t}\mathbf{B}'_j+\mathbf{\Psi}_j$. In this case smoothing is not needed due to the degenerate nature of the transition equation (6), and the updating equations are simply given by: $\mathbf{f}^j_{t|n_o}=\mathbf{f}^j_{t|t}$ and $\mathbf{H}^j_{t|n_o}=\mathbf{H}^j_{t|t}$.

2.2. The EM training

In this section, we describe an iterative approach for the estimation of the composite hidden Markov factor analysis model based on an extension of the EM algorithm called Variational-EM algorithm. Our algorithm alternates between two steps: optimizing an auxiliary function over the hidden Markovian states and the common latent factors (E-step) and optimizing the model parameters given the auxiliary function (M-step). In the first step we compute the expected log-likelihood given the complete data and the current model parameter estimates, using the factor estimates obtained by the switching Kalman filtering algorithm and the weightings $\xi^{(j)}_t$ obtained via the structured variational-based approach.[‡]

For composite hidden Markov factor analysis models, the parameters $\boldsymbol{\mu}_j$, $\mathbf{B}_j$ and $\mathbf{\Psi}_j$ can be computed directly, without any approximations. This is a weighted version of the updating formulae for the parameters of standard factor analysis models. Furthermore, the updating formulae for the initial state probability π_j and the transition probabilities p_{ij} are too similar to those obtained by the Baum-Welch algorithm for the simple hidden Markov model.

$$\widehat{\pi}_j=\frac{\xi^{(j)}_1}{\sum_{i=1}^{n_s}\xi^{(i)}_1}$$

$$\widehat{p}_{ij}=\frac{\sum_{t=2}^{n_o}\xi^{(i)}_{t-1}\xi^{(j)}_t}{\sum_{t=2}^{n_o}\xi^{(i)}_{t-1}}$$

The specific mean re-estimation formula is given by:

$$\widehat{\boldsymbol{\mu}}_j=\frac{\sum_{t=1}^{n_o}\xi^{(j)}_t\left(\mathbf{r}_t-\mathbf{B}_j\mathbf{f}^j_{t|n_o}\right)}{\sum_{t=1}^{n_o}\xi^{(j)}_t}$$

and the l-th factor loadings line of the matrix $\mathbf{B}_j$ by:

$$\widehat{\mathbf{b}}_{jl}=\left[\sum_{t=1}^{n_o}\xi^{(j)}_t(r_{tl}-\mu_{jl})\mathbf{f}^j_{t|n_o}\right]'\left[\sum_{t=1}^{n_o}\xi^{(j)}_t\left[\mathbf{H}^j_{t|n_o}+\mathbf{f}^j_{t|n_o}\mathbf{f}^{j\prime}_{t|n_o}\right]\right]^{-1}$$

[‡]More details about the variational procedure and the weights $\xi^{(j)}_t$ are available in Saidane and Lavergne (2007a)

where r_{tl} is the *l*-th crypto asset's time t log-return and μ_{jl}, the corresponding specific mean in the market regime j.

Finally the updated idiosyncratic covariance matrix is given by:

$$\widehat{\mathbf{\Psi}}_j = \frac{\sum_{t=1}^{n_o} \xi_t^{(j)} diag\left\{\mathbf{r}_t\mathbf{r}_t' - A_{jt|n_o} - A_{jt|n_o}' + M_{jt|n_o}\right\}}{\sum_{t=1}^{n_o} \xi_t^{(j)}}$$

where

$$A_{jt|n_o} = \left[\begin{array}{cc} \mathbf{B}_j & \boldsymbol{\mu}_j \end{array}\right] \left[\begin{array}{c} \mathbf{f}_{t|n_o}^j \mathbf{r}_t' \\ \mathbf{r}_t' \end{array}\right]$$

and

$$\mathbf{M}_{jt|n_o} = \left[\begin{array}{cc} \mathbf{B}_j & \boldsymbol{\mu}_j \end{array}\right] \left[\begin{array}{cc} \mathbf{H}_{t|n_o}^j + \mathbf{f}_{t|n_o}^j \mathbf{f}_{t|n_o}^{j\prime} & \mathbf{f}_{t|n_o}^j \\ \mathbf{f}_{t|n_o}^{j\prime} & 1 \end{array}\right] \left[\begin{array}{c} \mathbf{B}_j' \\ \boldsymbol{\mu}_j' \end{array}\right]$$

In all the above formulae, $\xi_t^{(j)}$ are the responsibilities assigned to the log-return vector $\mathbf{r}_t$ under market regime j.

In the second step, given the updated estimates of π_j, p_{ij}, $\boldsymbol{\mu}_j$, $\mathbf{B}_j$ and $\mathbf{\Psi}_j$, and the approximation established by Harvey, et al., (1992):

$$\mathbf{r}_t|\mathcal{R}_{1:t-1}, S_t = j, \mathcal{S}_{1:t-1} \approx \mathcal{N}\left[\boldsymbol{\mu}_j, \mathbf{\Omega}_{t|t-1}^j\right]$$

we get the following result:

$$\mathbf{\Omega}_{t|t-1}^j = \mathbf{B}_j \mathbf{H}_{t|t-1}^j \mathbf{B}_j' + \mathbf{\Psi}_j$$

where $\mathbf{H}_{t|t-1}^j$ is the expected value of $\mathbf{H}_t$, given the time $t-1$ information set, computed by the quasi-optimal switching Kalman filter algorithm developed in Saidane and Lavergne (2007b, 2008). In this case, the parameters $a_j = \{a_{1jl}, a_{2jl}, a_{3jl}, a_{4jl}\}$ for $j = 1, ..., n_s$ can be updated through the maximization of the observed log-likelihood function:

$$\mathcal{L}^* = c - \frac{1}{2}\sum_{t=1}^{n_o}\sum_{j=1}^{n_s} \xi_t^{(j)} \left[\log|\mathbf{\Omega}_{t|t-1}^j| + (\mathbf{r}_t - \boldsymbol{\mu}_j)'\mathbf{\Omega}_{t|t-1}^{j\,-1}(\mathbf{r}_t - \boldsymbol{\mu}_j)\right] \tag{7}$$

To solve the above nonlinear optimization problem, we can use the R-package `NlcOptim` developed by Chen and Yin (2019) after identifying the optimal hidden process.

The EM Algorithm

Initialization of the model parameters.[§]

E step (We repeat these iterations until convergence of the $KL(Q\|p)$)

1. Computation of $q_t^{(j)}$ based on the prediction errors of model j.
2. Computation of $\xi_t^{(j)}$ using forward-backward recursions and the probabilities $q_t^{(j)}$.
3. Running the Kalman filter, with data weighted by $\xi_t^{(j)}$.

M step

1. Updating the model parameters using data weighted by $\xi_t^{(j)}$.
2. Updating the Markov process parameters with the Baum-Welch procedure.
3. Updating the common variance parameters using the `NlcOptim` R-package.

3. Crypto asset allocation strategies and risk assessment

Let $\mathbf{r}_t$ be the q-dimensional vector of log-returns on the q cryptocurrencies at time t. The dynamic asset allocation theory assumes that an investment in the different currencies at each time t can be reallocated for the next period $t+1$ according to a portfolio $\mathcal{P}_{t+1}$. Thus, the amounts of American dollars (USD) invested in the different currencies are given in the vector $\mathcal{P}_{t+1}$.

In this paper no transaction costs are assumed and the amounts of USD may be reallocated freely and instantaneously to arbitrary short or long positions across the different cryptocurrencies, subject initially only to the constraint $\mathcal{P}_t'\mathbf{1} = 1$, where $\mathbf{1}$ is the unity vector. The choice of the best model over a chosen time interval can be done based on the cumulative returns given by the USD amount $r_t^* = \mathcal{P}_t'\mathbf{r}_t$ (the realized return of the portfolio at time t).

3.1. Dynamic portfolio optimization across hidden market regimes

The Markowitz's (1952) portfolio model is based on the concept of diversification. Thus, the different assets composing a portfolio at each time t cannot be selected individually and must be chosen according to the predicted correlation of their returns with those of the other assets. This selection process allows to minimize the portfolio variance given an expected rate of return.

For the implementation of the different dynamic allocation strategies we need the predicted correlation matrix, as well as, the expected return vector, which may be computed using our composite hidden Markov model and the other baseline models. In the case of the CHMFA model, the predicted mean vector $\boldsymbol{\mu}_{t+1|t}$ and covariance matrix $\boldsymbol{\Omega}_{t+1|t}$ of the log-return vector $\mathbf{r}_t$ can be computed as follows:

$$\boldsymbol{\mu}_{t+1|t} = \mathbb{E}(\mathbf{r}_{t+1}|\mathcal{D}_{1:t}) = \boldsymbol{\mu}_j \tag{8}$$

and

$$\boldsymbol{\Omega}_{t+1|t} = Var(\mathbf{r}_{t+1}|\mathcal{D}_{1:t}) = \mathbf{B}_j\mathbf{H}_{t+1|t}^{(j)}\mathbf{B}_j' + \boldsymbol{\Psi}_j \tag{9}$$

where

$$\mathbf{H}_{t+1|t}^{(j)} = diag\left[\widetilde{h}_{lt+1|t}^{(j)}\right]_{l=1,\ldots,k}$$

[§]For more details on the variational parameters $q_t^{(j)}$, $\xi_t^{(j)}$ and the minimization of the Kullback-Leibler divergence $KL(Q\|p)$, one can refer to Saidane and Lavergne (2007a).

and $\forall j = 1, ..., n_s$,

$$\begin{aligned}\widetilde{h}_{lt+1|t}^{(j)} &= a_{1jl} + a_{2jl}\mathbb{E}(f_{lt}^{(i)}|\mathcal{D}_{1:t}) + a_{3jl}\mathbb{E}(f_{lt}^{(i)\,2}|\mathcal{D}_{1:t}) + a_{4jl}\mathbb{E}(h_{lt}^{(i)}|\mathcal{D}_{1:t}) \\ &= a_{1jl} + a_{2jl}f_{lt|t}^{(i)} + a_{3jl}f_{lt|t}^{(i)\,2} + a_{4jl}h_{lt|t}^{(i)}\end{aligned}$$

In this case, the predicted conditional volatilities of the different crypto assets $\omega_{l,t+1|t}^{(j)}$ are given by the diagonal elements of the covariance matrix (9) and the optimal future state can be identified as follows:

$$S_{t+1|t}^{*} = \arg\max_{j} p(S_{t+1} = j|\mathcal{R}_{1:t}; \Theta), \quad 1 \leq t \leq n_o - 1$$

where Θ denotes the set of the model parameters. In this case, the posterior probabilities maximized by $S_{t+1|t}^{*}$ are given by:

$$\begin{aligned}p(S_{t+1} = j|\mathcal{R}_{1:t}) &= \sum_{i=1}^{n_s} P(S_{t+1} = j, S_t = i|\mathcal{R}_{1:t}) \\ &= \frac{\sum_{i=1}^{n_s} p(\mathcal{R}_{1:t}|S_{t+1} = j, S_t = i)p(S_{t+1} = j, S_t = i)}{p(\mathcal{R}_{1:t})} \\ &= \frac{\sum_{i=1}^{n_s} p(\mathcal{R}_{1:t}, S_t = i)p_{ij}}{p(\mathcal{R}_{1:t})} \\ &\approx \sum_{i=1}^{n_s} \xi_t^{(i)} p_{ij}\end{aligned}$$

where $\xi_t^{(i)}$ are the responsibilities assigned to factor model i for the observation vector $\mathbf{r}_t$.

Our dynamic optimization problem consists at each time t to find the optimal allocation strategy by minimizing the portfolio's risk for a certain expected return value:

$$\begin{cases} \arg\min\limits_{\mathcal{P}_{t+1}} \left\{\mathcal{P}_{t+1}'\mathbf{\Omega}_{t+1|t}\mathcal{P}_{t+1}\right\} \\ \quad \text{s.t } \mathcal{P}_{t+1}'\boldsymbol{\mu}_{t+1|t} = m \\ \quad\quad \text{and } \mathcal{P}_t'\mathbf{1} = 1 \end{cases} \tag{10}$$

In this case, we call efficient frontier (curve) the set of all portfolios that minimize the risk subject to a predefined expected return. The mean-variance optimal (efficient) portfolio $\mathcal{P}_{t+1}^{(m)}$ is the solution to the quadratic optimization system (10), which can be obtained as follows:

$$\mathcal{P}_{t+1}^{(m)} = \mathbf{\Omega}_{t+1|t}^{-1}(\lambda\boldsymbol{\mu}_{t+1|t} + \delta\mathbf{1}) \tag{11}$$

where

$$\lambda = \mathbf{1}'\mathbf{\Omega}_{t+1|t}^{-1}e$$

and

$$e = \frac{(\mathbf{1}m - \boldsymbol{\mu}_{t+1|t})}{d}$$

and

$$d = (\mathbf{1}'\boldsymbol{\Omega}_{t+1|t}^{-1}\mathbf{1})(\boldsymbol{\mu}_{t+1|t}'\boldsymbol{\Omega}_{t+1|t}^{-1}\boldsymbol{\mu}_{t+1|t}) - \left(\mathbf{1}'\boldsymbol{\Omega}_{t+1|t}^{-1}\boldsymbol{\mu}_{t+1|t}\right)^2$$

Two other allocation solutions can also be obtained by solving the previous quadratic system. The first one, depending only on the predicted covariance matrix, called strictly risk-averse strategy, is given by:

$$\mathcal{P}_{t+1}^{(mv)} = \left(\mathbf{1}'\boldsymbol{\Omega}_{t+1|t}^{-1}\mathbf{1}\right)^{-1}\boldsymbol{\Omega}_{t+1|t}^{-1}\mathbf{1} \tag{12}$$

The second one, called target-independent strategy, is centered on the boundary of the efficient curve:

$$\mathcal{P}_{t+1}^{(me)} = \left(\mathbf{1}'\boldsymbol{\Omega}_{t+1|t}^{-1}\boldsymbol{\mu}_{t+1|t}\right)^{-1}\boldsymbol{\Omega}_{t+1|t}^{-1}\boldsymbol{\mu}_{t+1|t} \tag{13}$$

Finally, we note that there are many other extensions of the basic strategies (11-13). For example, if we allow for short and long investment positions by removing all the resources constraints imposed on the vector $\mathcal{P}_{t+1}$, we obtain the unconstrained targeted mean efficient portfolio corresponding to a given expected return m, as follows:

$$\mathcal{P}_{t+1}^{(*m)} = \frac{m\boldsymbol{\Omega}_{t+1|t}^{-1}\boldsymbol{\mu}_{t+1|t}}{\left(\boldsymbol{\mu}_{t+1|t}'\boldsymbol{\Omega}_{t+1|t}^{-1}\boldsymbol{\mu}_{t+1|t}\right)} \tag{14}$$

In section 4, all these dynamic allocation strategies (11-14) will be used in conjunction with the different competing models in order to evaluate the forecasting accuracy of these models, as well as, their ability to measure the risk associated with cryptocurrency portfolios.

3.2. Sequential VaR and ES computations

In this section, we follow a similar methodology to that detailed in Saidane (2022b) for the computation of the VaR and ES risk measures. Monte Carlo simulations are performed in a rolling window scheme using $N_{ms} = 25.000$ random scenarios, to achieves a balance between accuracy and efficiency. The steps of the Monte-Carlo approach, based on the simulation of random scenarios from the composite hidden Markov factor analysis model, are detailed as follows:

Step 1: A loss probability level $\alpha\%$ for the VaR measure is chosen.
Step 2: N_{ms} different random scenarios are simulated from the predictive distribution of the conditionally heteroskedastic latent factors $\mathbf{f}_{t+1|t}^s$ with the highest variational parameter, $\xi_t^{(j)}$, as follows:

(a) Standardized factors $\mathbf{f}_t^*$ are first simulated from $\mathcal{N}(0, I_k)$.
(b) Thereafter, the Cholesky decomposition of $\mathbf{H}_{t+1|t}^{(j)}$ is used to find the lower triangular matrix $\mathbf{H}_{t+1|t}^{(j)*}$ and to calculate

$$\mathbf{f}_{t+1|t}^s = \mathbf{H}_{t+1|t}^{(j)*}\mathbf{f}_t^*$$

Step 3: N_{ms} different random scenarios are simulated from the predictive distribution of the idiosyncratic factors $\boldsymbol{\epsilon}_{t+1|t}^s$ with the highest variational parameter, $\xi_t^{(j)}$, as follows:

(a) Standardized factors $\boldsymbol{\epsilon}_t^*$ are first simulated from $\mathcal{N}(0, I_q)$.
(b) Thereafter, the Cholesky decomposition of $\boldsymbol{\Psi}_j$ is used to find the lower triangular matrix $\boldsymbol{\Psi}_j^*$ and to calculate

$$\boldsymbol{\epsilon}^{s}_{t+1|t} = \boldsymbol{\mu}_j + \boldsymbol{\Psi}^{*}_j \boldsymbol{\epsilon}^{*}_t$$

Step 4: N_{ms} portfolio return scenarios are simulated from the composite hidden Markov model, using the 4 dynamic allocation strategies (section 3.1), as follows:

$$\begin{aligned}
\mathcal{R}^{m}_{t+1|t} &= \mathcal{P}^{m}_{t+1}{}' \mathbf{r}^{s}_{t+1|t} \\
\mathcal{R}^{mv}_{t+1|t} &= \mathcal{P}^{mv}_{t+1}{}' \mathbf{r}^{s}_{t+1|t} \\
\mathcal{R}^{me}_{t+1|t} &= \mathcal{P}^{me}_{t+1}{}' \mathbf{r}^{s}_{t+1|t} \\
\mathcal{R}^{*m}_{t+1|t} &= \mathcal{P}^{*m}_{t+1}{}' \mathbf{r}^{s}_{t+1|t}
\end{aligned}$$

where

$$\mathbf{r}^{s}_{t+1|t} = \mathbf{B}_j \mathbf{f}^{s}_{t+1|t} + \boldsymbol{\epsilon}^{s}_{t+1|t}$$

Step 5: In this step, we ignore the portion of the $\alpha\%$ worst simulated returns. The predicted VaR measure at time t, for each allocation strategy, is calculated as the minimum of the remaining simulated returns. The predicted ES, called also conditional VaR, is calculated as the mean value of the loss exceeding VaR. In this case, the ES can be interpreted as the average loss in the worst $\alpha\%$ of cases.

4. Data and empirical findings

The main focus of this paper is the use of the composite hidden Markov factor analysis model to predict the VaR and ES in a crypto-portfolio context. Our dataset downloaded from the "Yahoo Finance" website[¶], consists of the closing prices listed in US dollars of the six most popular cryptocurrencies, namely the Bitcoin (BTC), Litecoin (LTC), DASH, Ethereum (ETH), Ripple (XRP), and the Stellar (XLM) currencies. The dataset covers the period from October 01, 2018 until September 30, 2022 (i.e. 1460 daily returns).

Cryptocurrencies' prices are driven by a supply and demand process without any dividend distribution mechanism. In this case, they can be modeled as a geometric Brownian motion process, and the realized volatility proposed by Alizadeh et al. (2002) can also provide a good proxy measure for the true observed volatility.

The forecasting performance of our methodology is evaluated here by applying the one-day rolling window approach (see Saidane, 2022a). The dataset is divided into a training set with observations from October 01, 2018, to September 30, 2019 (365 log-returns), on which we train and estimate the parameters of our composite hidden Markov model and those of other baseline prediction methods presented in the literature, such as: the standard factor analyzed hidden Markov model (FAHMM) (Saidane and Lavergne, 2006), the switching dynamic state-space model (SSSM) (Saidane and Lavergne, 2009), the conditionally heteroskedastic latent factor model (CHFM) (Saidane, 2017, 2023) and the mixed factorial HMM (MFHMM) (Saidane, 2019).

On the prediction set, we compute a one-step ahead out-of-sample forecast for the mean and the volatility of the first trading day of October 2019, using the different models. Thereafter, the realized log-returns for October 1, 2019 are added and those of 2018 are dropped from the training set and the different models are again estimated and used to predict the mean and the volatility of the next trading day. This process continues until we obtain mean and volatility predictions from October 01, 2019 to September 30, 2022 (1095 daily predictions).

In order to select the optimal model that will ensure the most probable forecast, we run different configurations (by varying the number of common latent factors and HMM states), using the maximum likelihood principle on the rolling-window data sample (a window size of 365 trading days). Minimizing the Schwarz's (1978) or BIC criterion - calculated after each EM implementation - enables us to obtain the optimal model among all possible sub-models. The same procedure is performed for all the other competing models.

[¶]https://finance.yahoo.com/crypto/

4.1. Data description

Table 1 reports some summary statistics for the six cryptocurrency daily return series on the period ranging from October 01, 2018 to September 30, 2022. Returns are calculated as log-differences between closing prices.

Table 1. Descriptive statistics for the daily cryptocurrency log-returns from 01/10/2018 to 30/09/2022.

	Cryptocurrency					
Statistic	BTC	LTC	DASH	ETH	XRP	XLM
Mean	0.00148	0.00129	0.00067	0.00244	0.00153	0.00099
Std. Dev.	0.0380	0.0521	0.0588	0.0493	0.0583	0.0572
Min	-0.3717	-0.3618	-0.3721	-0.4235	-0.4233	-0.3363
Q_3	0.0177	0.0260	0.0248	0.0269	0.0199	0.0239
Med.	0.00108	0.00042	0.00068	0.00156	-0.00062	-0.00067
Q_1	-0.0150	-0.0253	-0.0250	-0.0207	-0.0216	-0.0263
Max	0.1875	0.3083	0.5704	0.2595	0.5601	0.7492
Skewness	-0.4048	-0.1254	1.1563	-0.3613	1.3406	2.1367
Kurtosis	11.710	8.7233	17.477	9.3983	19.343	29.802
BJ test	4655.5	1996.5	13074	2522.2	16685	44811
p-values	(0.0000)	(0.0000)	(0.0000)	(0.0000)	(0.0000)	(0.0000)
LB(1)	141.83	135.76	127.98	116.46	131.70	128.56
p-values	(0.0178)	(0.0191)	(0.0218)	(0.0236)	(0.0204)	(0.0211)

From this table we can see that the empirical skewness is larger than 1 for the DASH, XRP and XLM currencies and negative for the other currencies. On the other hand, the empirical kurtosis for all the return series are greater than 3, with the smallest kurtosis corresponding to the LTC returns (8.7233) and the largest to the XLM (29.802). This indicates that all the log-returns have skewed and leptokurtic distributions and deviate from the normal distribution assumption. Furthermore, the *p*-values of the Bera and Jarque (1982) BJ test are all very small (< 0.0001), which confirm that all the crypto asset log-return are not normally distributed. From this table, we can see also that all the *p*-values of the Ljung and Box (1978) LB(1) test for the squared return of the crypto asset prices are very low, so we reject the null hypothesis of absence of first order correlation. Following Bollerslev (1987), we can interpret the presence of significant correlations between the squared returns as a sign of volatility clustering, which imply that small (large) changes in volatility tend to be followed by small (large) ones and can be modeled and predicted using conditional heteroskedastic family models.

All the crypto asset closing prices, together with their corresponding log-returns are plotted in Figure 1. This figure shows a strong evidence of serial correlation in the data and a persistence in the conditional variances of the different series.

We note finally that the sample correlation coefficients are fairly large for the pairs BTC-LTC (0.7941), BTC-ETH (0.8200), LTC-ETH (0.8259), DASH-LTC (0.7261) and XRP-XLM (0.7239). These results imply a possibility of a strong comovement between all the crypto asset log-returns. In this case, a multivariate Markov-switching factorial approach with time-vaying volatility seems to be more suitable for modeling and forecasting the VaR and ES of cryptocurreny portfolios during crisis periods.

4.2. Forecasting strategy and performance metrics

In order to examine the prediction performance of our CHMFA approach and the other benchmark models, we used four accuracy metrics: the mean absolute error (MAE), the mean square error (MSE) and the Theil-U statistic. We used also the "correct directional change" (CDC) metric, which evaluates the aptitude of each model to correctly forecast the next trading day's movement direction in volatility. These metrics are given by the following formulas:

$$\text{MAE} = \frac{1}{n}\sum_{t=1}^{n}\left|\sigma_t^2 - \widehat{\sigma}_t^2\right| \tag{15}$$

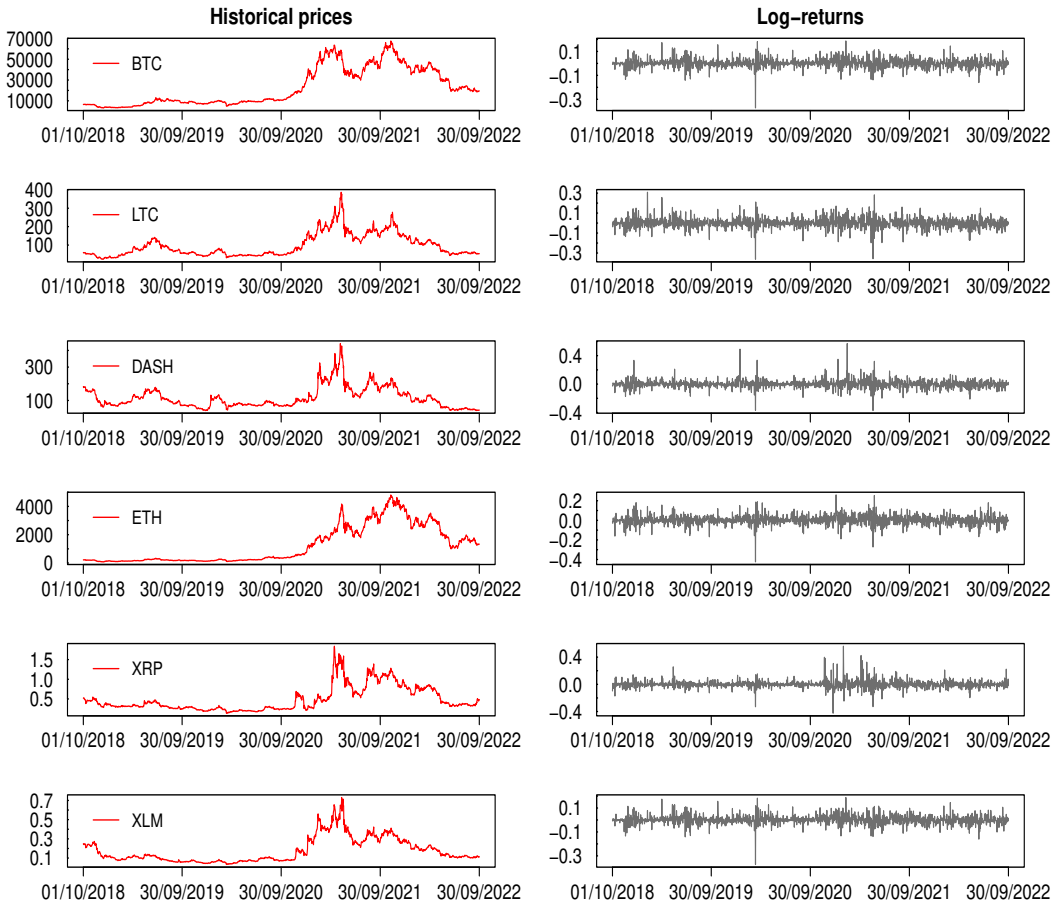

Figure 1. The cryptocurrency historical prices and their corresponding log-returns for the period 01-10-2018 - 30-09-2021.

$$\text{MSE} = \frac{1}{n}\sum_{t=1}^{n}\left(\sigma_t^2 - \widehat{\sigma}_t^2\right)^2 \tag{16}$$

$$\text{Theil-U} = \frac{\sum_{t=2}^{n}\left(\widehat{\sigma}_t^2 - \sigma_t^2\right)^2}{\sum_{t=2}^{n}\left(\sigma_t^2 - \sigma_{t-1}^2\right)^2} \tag{17}$$

$$\text{CDC} = \frac{1}{n}\sum_{t=1}^{n} d_t \quad \text{where} \quad d_t = \begin{cases} 1 & \text{if } (\sigma_t^2 - \sigma_{t-1}^2)\cdot(\widehat{\sigma}_t^2 - \widehat{\sigma}_{t-1}^2) \geq 0 \\ 0 & \text{otherwise} \end{cases} \tag{18}$$

MAE is the mean of absolute differences between pairs of predicted volatilities $\widehat{\sigma}_t^2$ obtained from the different models and actual volatilities σ_t^2. MSE is the mean of squared differences between actual and predicted volatilities. The Theil-U statistic is the ratio of the mean squared prediction error of our models to that from a random walk prediction. The advantage of this metric is that it is independent from the variable's scale. Theil-U's less than 1

Table 2. Forecasting accuracy of the different models for the period October 01, 2019-September 30, 2022.

		Model				
Currency	Statistic	CHFM	FAHMM	SSSM	MFHMM	CHMFA
BTC	MAE	0.0477	0.0512	0.0428	0.0456	0.0407
	MSE	0.00838	0.00953	0.00752	0.00774	0.00682
	Theil-U	1.621	1.689	0.592	0.611	0.548
	CDC	66.72%	68.18%	79.44%	74.83%	85.52%
LTC	MAE	0.0382	0.0406	0.0341	0.0360	0.0276
	MSE	0.00726	0.00843	0.00671	0.00692	0.00594
	Theil-U	1.544	1.282	0.430	0.447	0.388
	CDC	67.21%	70.01%	80.62%	76.11%	88.17%
DASH	MAE	0.0572	0.0594	0.0516	0.0548	0.0493
	MSE	0.00871	0.00926	0.00741	0.00778	0.00715
	Theil-U	1.079	0.931	0.557	0.589	0.528
	CDC	64.19%	66.46%	83.04%	80.42%	87.85%
ETH	MAE	0.0461	0.0477	0.0398	0.0428	0.0366
	MSE	0.00573	0.00590	0.00462	0.00498	0.00427
	Theil-U	1.633	0.889	0.609	0.616	0.588
	CDC	73.26%	76.75%	90.71%	87.34%	96.74%
XRP	MAE	0.0170	0.0169	0.0157	0.0154	0.0161
	MSE	0.00579	0.00585	0.00484	0.00561	0.00473
	Theil-U	1.685	1.571	0.568	0.564	0.561
	CDC	74.56%	72.33%	89.76%	86.17%	91.97%
XLM	MAE	0.0234	0.0248	0.0172	0.0189	0.0133
	MSE	0.00499	0.00522	0.00481	0.00496	0.00450
	Theil-U	1.584	1.593	0.567	0.579	0.534
	CDC	70.68%	74.03%	92.56%	88.32%	95.44%

indicate relatively improved prediction accuracy against the naive random walk benchmark; whereas values greater than 1 indicate poor prediction performance.

Notice here that all the considered metrics are useful for measuring forecasting accuracy, but they doesn't consider the prediction's direction (say, positive or negative). However, many trading strategies rely on the prediction of the direction of volatility rather than its level. In this case, the CDC, as a measure of the direction change accuracy, addresses this issue.

All the results obtained for the different models on the out-of-sample period, from 01/10/2019 to 30/09/2022, are given in Table 2. From this table, we can see that Theil-U's are generally greater than 1 for the CHFM and FAHMM models, and less than 1 for the other models. We can see also, from the MSE values, the significant superiority in terms of prediction ability of our CHMFA model with respect to the other competing models for the different volatility series. On the other hand, based on the MAE results, we see that the MFHMM gives significantly better forecasts than those obtained by the other models for the the XRP volatility. From the Theil-U metric results we can argue that the only model which does not perform better than the random walk is the CHFM. In this case, the Theil-U value is larger than one for all the cryptocurrencies considered.

In general, our composite hidden Markov factor analysis model performs better than the other competing models in all of the three metrics. It gives also, the most accurate directional change predictions for all the cryptocurrency volatilities. The switching dynamic state-space model is ranked second.

4.3. The encompassing test

Despite their usefulness, the prediction evaluation measures used previously cannot determine if the forecasting power of a model is "significantly" better or worse than another. In order to assess the forecasting superiority of a model over a given benchmark, we will follow the forecast-encompassing approach proposed by Harvey, et al., (1998). In this case, when a model $\mathcal{M}^*$ gives useful information that is not contained in the benchmark $\mathcal{M}$, we say that the first model encompasses the second one. For more details on the implementation of this test and more applications with financial data, in a rolling window framework, one can refer to Saidane and Lavergne (2011, 2009).

Table 3. Results of the encompassing tests for the BTC, LTC and DASH data on the period October 01, 2019-September 30, 2022.

		Forecast $\widehat{\sigma}^2_{kt}$ from $\downarrow$				
Currency	Forecast error $\sigma^2_{jt} - \widehat{\sigma}^2_{jt}$ from $\downarrow$	CHFM	FAHMM	SSSM	MFHMM	CHMFA
BTC	CHFM	NA	0.2783	0.0324	0.0428	0.0206
	FAHMM	0.0460	NA	0.0311	0.0394	0.0212
	SSSM	0.4163	0.4810	NA	0.3376	0.0379
	MFHMM	0.1104	0.6231	0.0348	NA	0.0243
	CHMFA	0.6352	0.7106	0.0431	0.6602	NA
LTC	CHFM	NA	0.3172	0.0381	0.0336	0.0229
	FAHMM	0.0411	NA	0.0488	0.0372	0.0247
	SSSM	0.5270	0.5206	NA	0.4617	0.0631
	MFHMM	0.1857	0.4913	0.0314	NA	0.0305
	CHMFA	0.6118	0.6780	0.1196	0.7142	NA
DASH	CHFM	NA	0.4207	0.0406	0.0389	0.0337
	FAHMM	0.0462	NA	0.0461	0.0388	0.0381
	SSSM	0.6854	0.6371	NA	0.6608	0.0402
	MFHMM	0.3722	0.5704	0.0394	NA	0.0387
	CHMFA	0.6429	0.6208	0.4321	0.6934	NA

Tables 3 and 4 summarize the results of this test for the individual cryptocurrency volatility series. The model forecast (independent variable), is given at the top of the tables and the model prediction error (dependent variable) is given down the left side of the tables. The *p*-values of the regression coefficients used in this test are given in the entries of the tables. In this case, a *p*-value less than 0.05 means that the prediction from the corresponding model given at the top of the table explains the prediction error from the corresponding model given down the left side of the table, and this result imply that the second model cannot encompass the first one.

From Table 3, we can see that the *p*-values related to the LTC currency are all greater to the significance level 5% in the SSSM and CHMFA rows. These results indicate that the prediction errors of these models are not explained by any other model's forecasts, which in turn imply that these models are not encompassed by any of the other competing models. We can see also that the forecasts obtained from the SSSM and CHMFA models can explain the prediction errors of the other benchmarks at the significance level of 5%. From here, we can conclude that the CHFM, FAHMM and MFHMM models are encompassed by the SSSM and our CHMFA framework.

The results in Table 3 also indicate that the prediction errors of our CHMFA for the BTC, LTC and DASH currencies are not explained by any other model's forecasts at the significance level of 5%. On the other hand, the forecasting errors of the competing models are significantly explained by the predictions obtained by our model (except for the LTC), which imply that our proposed framework encompasses in general all the competitors. Furthermore, the results for the ETH, XRP and XLM currencies reported in Table 4, confirm in turn that our CHMFA-based framework performs better than all the other competing forecasting models.

Table 4. Results of the encompassing tests for the ETH, XRP and XLM data on the period October 01, 2019-September 30, 2022.

		Forecast $\widehat{\sigma}^2_{kt}$ from $\downarrow$				
Currency	Forecast error $\sigma^2_{jt} - \widehat{\sigma}^2_{jt}$ from $\downarrow$	CHFM	FAHMM	SSSM	MFHMM	CHMFA
ETH	CHFM	NA	0.3815	0.0453	0.0481	0.0374
	FAHMM	0.0419	NA	0.0446	0.0327	0.0281
	SSSM	0.5503	0.5127	NA	0.4865	0.0422
	MFHMM	0.263	0.5922	0.0418	NA	0.0332
	CHMFA	0.6824	0.7452	0.5301	0.7110	NA
XRP	CHFM	NA	0.3824	0.0428	0.0317	0.0388
	FAHMM	0.0486	NA	0.0455	0.0424	0.0391
	SSSM	0.5608	0.5881	NA	0.5772	0.0347
	MFHMM	0.3851	0.5115	0.0461	NA	0.0362
	CHMFA	0.6463	0.6240	0.3443	0.6673	NA
XLM	CHFM	NA	0.5874	0.0462	0.0419	0.0308
	FAHMM	0.0421	NA	0.0407	0.0449	0.0324
	SSSM	0.6307	0.6011	NA	0.6224	0.0396
	MFHMM	0.4853	0.5537	0.0465	NA	0.0343
	CHMFA	0.6159	0.6045	0.1484	0.7254	NA

Note finally, that all these results show that the SSSM and the CHMFA oftentimes encompass the other competing prediction models. Our CHMFA model is never encompassed by the other models, whereas all the rival model are encompassed at least once. Hence, our framework, which nests the CHFM and FAHMM outperforms, in terms of encompassing tests, all benchmark approaches.

4.4. Empirical comparisons of the different portfolio strategies

In this section, all the comparisons will be conducted on the basis of the forecasting accuracy of the different competing models, using the dynamic allocation strategies presented in the previous section. Like the approach developed by Levy and Lopes (2021a), our sequential strategy allows to update the parameters of the model and to predict the future volatility, simultaneously. Levy and Lopes (2021b) have proposed an analogous procedure based on the dynamic factor risk model, but without any regime change.

In order to permit out-of-sample forecasting comparisons, the entire period from 01/10/2018 to 30/09/2022 is divided into training and forecasting periods. On the training set, from 01/10/2018 to 30/09/2019 (365 observations), we fitted our CHMFA model and the other baseline models to the daily cryptocurrency log-returns. Then, we used the 4 dynamic portfolio allocation strategies to assess the (one-step ahead) forecasting accuracy of the different models on the forecasting period, from 01/10/2019 to 30/09/2022 (1095 predictions).

The performance, in terms of cumulative returns, of the different models and the different allocation strategies are evaluated here through the one-day rolling window methodology. In Figure 2, we depict the cumulative return paths of the different dynamic strategies (with a predefined target daily return $m = 0.002$) used in conjunction with our BIC-optimal CHMFA model and the other BIC-optimal competing models. We can see clearly from this figure the dominance of our composite hidden Markov model for the different portfolio strategies.

According to the results of the previous encompassing tests and the cumulative returns given in Figure 2, we can affirm that the shifts in the volatility dynamics are much better detected by our CHMFA model. The SSSM is the "second classified" model. These models often give very close portfolio weights. In terms of cumulative financial returns they dominate all the other benchmarks for the different allocation strategies, except in the unconstrained strategy case where the dynamic switching SSM dominates the other models for the period up to the end of 2020.

From Figure 2, we can see also the strong similarity in the portfolio cumulative return paths given by the CHMFA and SSSM models, in the case of the efficient mean-variance strategy. The most notable deviations appear during

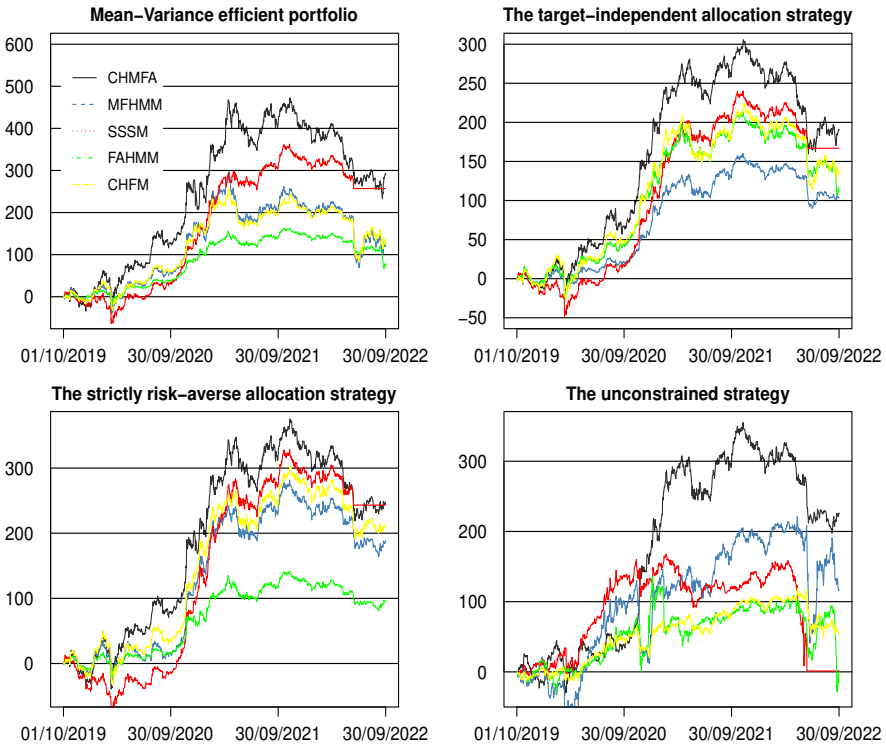

Figure 2. Cumulative returns, expressed in percentages, of the 4 dynamic allocation strategies).

periods of high volatility, where our CHMFA-based approach can capitalize more gains in the short-term than the switching dynamic SSM model. In the short term, the flexibility of our CHMFA model leads to high fluctuations in the weights of the cryptocurrency portfolios, that the constrained strategies can permanently capitalize on, resulting in a persistence of cumulative returns in the long term.

Figures 3-6 show the trajectories of the portfolio weights obtained by the optimal CHMFA model for the different dynamic allocation strategies. In this case, we used the target return $m = 0.002$. The plotted points are the relative portfolios weights, given by the real weights divided by $\mathbf{1}'\mathcal{P}_t$ and expressed in percentage terms. From these figures we can directly compare the constrained and unconstrained portfolio weights. In the constrained case, the real weights equal the relative ones. Through these figures we can see the significant fluctuations of the portfolio weights in response to the changes in the volatility regimes during 2022. As shown by Figure 2, these fluctuations have been translated into a considerable decrease in the cumulative financial returns during this period.

We can see from Figure 3 how the efficient mean-variance strategy turned rapidly in 2022 from long into short positions on the the DASH, XRP and XLM currencies. This figure shows also how this constrained strategy held long BTC and ETH positions for most of the time. Furthermore, we note that the specific mean related to the Bitcoin μ_1 is positive on the entire out-of-sample prediction period, which justifies the long positions (positive weights) on this currency (generally characterized by a low specific risk during this period) and confirms the previous results.

In relation with the previous results about the long positions on the Bitcoin, we can see from Figure 4 that the target-independent, as well as, the constrained allocation strategies adopt short positions on the DASH and XLM currencies. We note also that the BTC weights and those of the pair (DASH-XLM) globally compensate each other.

For the strictly risk-averse portfolio strategy with a minimum variance target, we can see from Figure 5 the small weights related to the DASH currency in almost the entire study period. These low weights can be explained by the DASH specific mean μ_3, which is very close to zero on average during this period. We note also that the specific

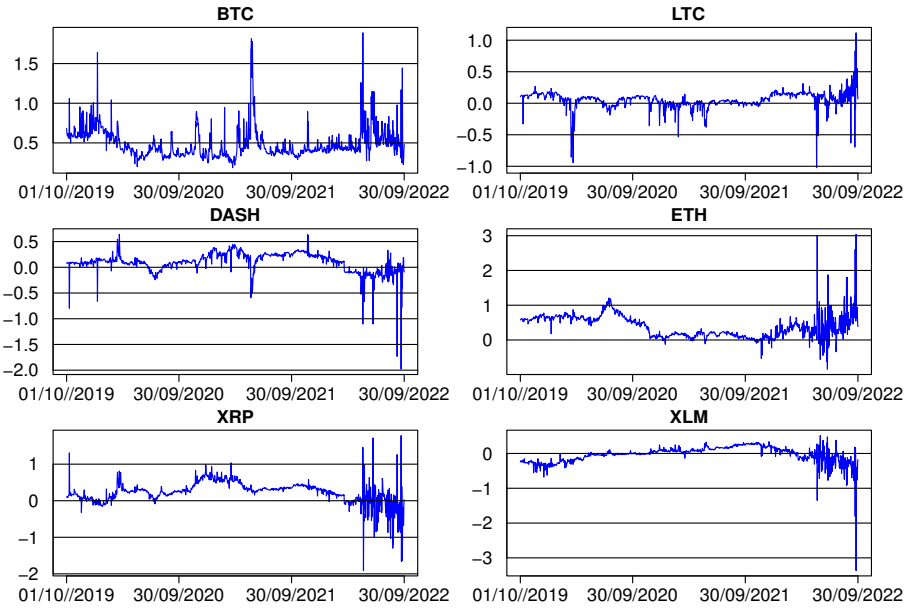

Figure 3. Dynamic weights $\mathcal{P}_t^{(m)}$ for the optimal mean-variance efficient strategy using the best CHMFA.

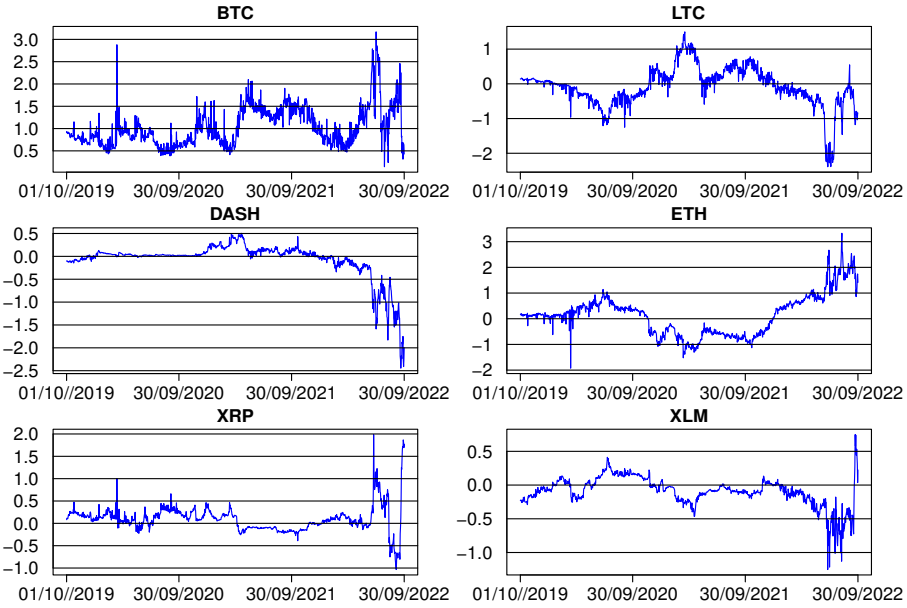

Figure 4. Dynamic weights $\mathcal{P}_t^{(me)}$ for the optimal target-independent strategy using the best CHMFA.

variance of the DASH was very high in this period, which explains the corresponding small weights in the portfolio and the high risk-aversion with regards to this currency during this period.

Indeed, when comparing figures 3 and 6, it is clear that the portfolio weight's trajectories of the optimal constrained mean-variance allocation strategy and the unconstrained strategy are very similar. We further notice

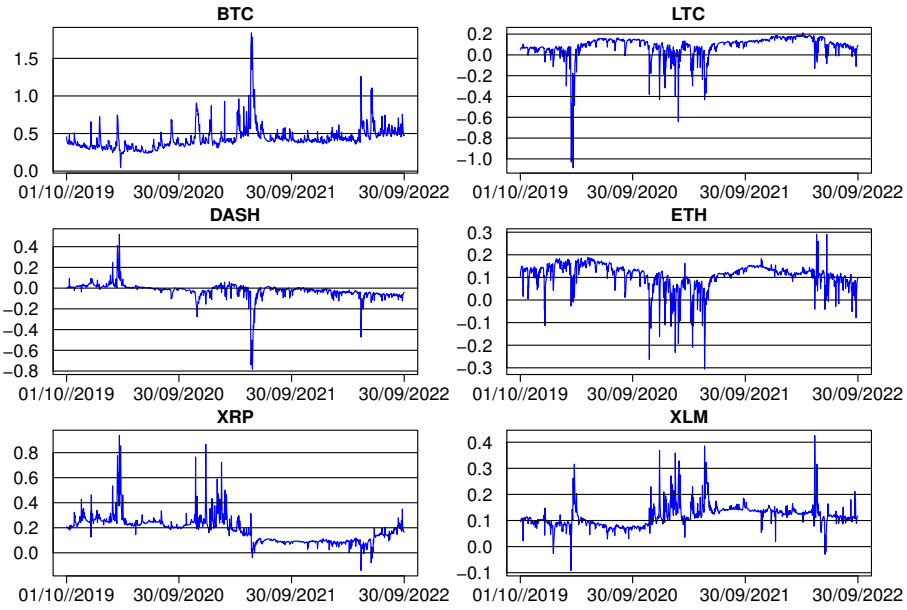

Figure 5. Dynamic weights $\mathcal{P}_t^{(mv)}$ for the optimal strictly risk-averse strategy using the best CHMFA.

that on the overall period, the unconstrained allocation strategies adopt long positions on the BTC, LTC, DASH and ETH currencies, which reflect the portfolio response to the low specific risk levels associated with these currencies.

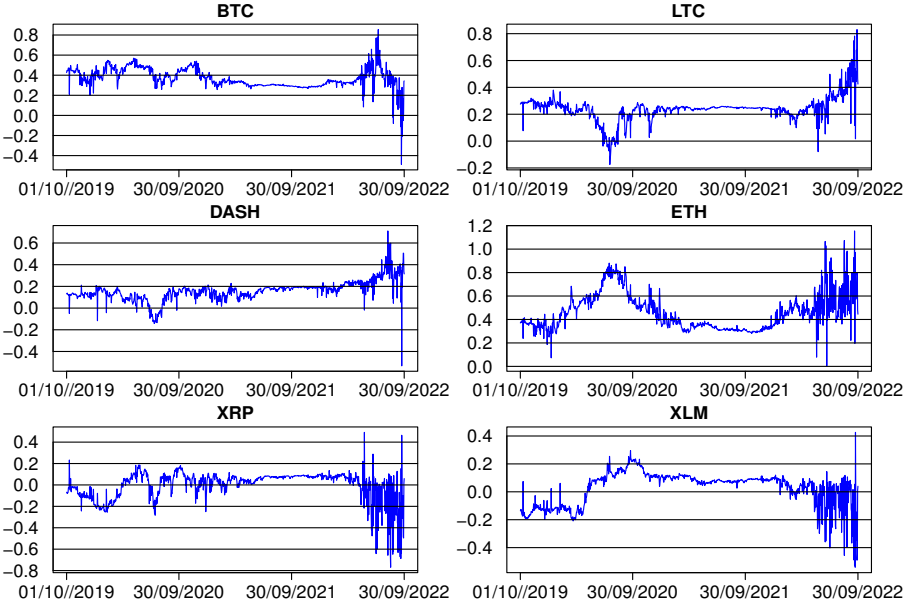

Figure 6. Dynamic weights $\mathcal{P}_t^{(*m)}$ for the mean efficient unconstrained strategy with target return $m = 0.002$, using the best CHMFA.

Finally, we note that although the cumulative returns given by the dynamic switching SSM are very close to those given by our CHMFA model during this period, the optimal portfolio weights obtained in this model were rather more stationary through time. In this case our model takes into account the switching dynamic correlations among various crypto asset returns and gives with the different allocation strategies more stationary weights than those obtained by the other competing baseline models.

4.5. Monte Carlo VaR and ES analysis

In this section we seek to identify the most suitable prediction model to evaluate the VaR and ES with the different dynamic crypto asset allocation strategies presented in section 3.1. For this reason, we estimated in a first time the latent correlation structure of the observed log-returns, directly from our composite hidden Markov factor analysis model and the other competing models. Thereafter, we followed the same one-day rolling window procedure used when evaluating the forecasting performance of our model. The training set contains observations from October 01, 2018, to September 30, 2019 (365 log-returns) and the backtesting set contains 1095 VaR and ES predictions (from October 01, 2019 to September 30, 2022).

To evaluate the accuracy of the VaR and ES predictions, in the out-of-sample period, we used a Monte Carlo-based simulation approach similar to that described in Saidane (2022b). In each backtesting step, the observed failure rates given by the different models for the significance levels 1%, 2%, 5% and 10% were recorded. Furthermore, for each allocation strategy, we computed the p-values of the Kupiec's (1995) unconditional coverage test (UC), the Christoffersen's (1998) independence (IND) and conditional coverage (CC) tests, the Engle and Manganelli (2004) dynamic quantile (DQ) test as well as the Gaglianone et al. (2011) VaR quantile (VQ) test.

Tables 5 and 6 report the percentage of observed returns smaller than the prdicted VaR (hits rates), as well as the p-values of the different tests. Results obtained for the Average Quantile Loss Function (AQL) of Gonzalez-Rivera et al. (2004) are also reported. When using a suitable VaR estimate, we expect to not reject the null hypothesis that means we have sufficient evidence to support the claim that the predicted hits rate is equal to the expected one and that the hits occur independently. Furthermore, we wish also a procedure that minimizes the distance between the daily realized returns and the predicted VaRs. In this case, the best approach among several alternative is the one which minimizes the AQL function.

For all the allocation strategies and the coverage rates 10% and 5%, only three models confirmed the null hypothesis that the predicted hits rate is equal to the expected one at the significance level 5%: the SSSM, the MFHMM and our CHMFA framework. Note that the CHFM, as well as the FAHMM, presented p-values smaller than 5% for most tests. Furthermore, following the approach developed by Hansen et al. (2011), we used a model confidence set-based technique (MCS) and we found a set of high-performance models with small quantile loss function. The results of these models are indicated in tables 5 and 6 in bold. According to these results, our model proved also to be superior to all the other competing models for the different dynamic allocation strategies.

For the Coverage rates 2% and 1%, the best model is the CHMFA and the second one is the SSSM which reported p-values larger than 5% for the UC and CC tests. Our results, show also the better quality of the best SSSM model compared to the optimal MFHMM for the coverage rates 5% and 2%. Furthermore, from the results of the CC, DQ and VQ tests, it appears that the optimal SSSM is more significant than the MFHMM model.

For the VaR 1%, our results show that only the CHMFA framework yielded p-values greater than 5% with the different allocation strategies. Hence our model seems the most satisfactory and gives the best VaR predictions for the different coverage rates. The second ranked model is the SSSM and the third one is the MFHMM.

Figures 7-8 display the VaR and ES for the different confidence levels using the optimal CHMFA with the 4 dynamic allocation strategies. A visual inspection shows that the behaviors of the predicted VaR and ES are strongly affected by volatility shocks. These conclusions, in turn, imply that the latent cross-correlations between the different crypto assets are directly related to the market volatility fluctuations. All these results are consistent with the values of the AQL function reported in Tables 5 and 6. Furthermore, the Hits rates given in tables 5 and 6, confirm also the strong dependency between the VaR violations and the significant fluctuations in the market volatility during this period. In this case, we can argue that the poor results given by the CHFM and FAHMM methods are due to the fact that the correlations between the different crypto asset returns are subject to changes in regime and are sensitive both to the level of volatility and its regime (high or low), but these models do not take

Table 5. Results of the backtesting experiments using different models and different allocation strategies for the confidence levels 90% and 95% on the period October 01, 2019-September 30, 2022.

		VaR 10%							VaR 5%						
Model	$\mathcal{P}_t$	% Hits	UC	IND	CC	DQ	VQ	AQL	% Hits	UC	IND	CC	DQ	VQ	AQL
CHFM	$\mathcal{P}_t^{(m)}$	12.5114	0.0792	0.1304	0.0489	0.2082	0.0550	0.8446	7.5800	0.0327	0.2081	0.0685	0.1868	0.0465	0.8676
	$\mathcal{P}_t^{(me)}$	12.4201	0.0310	0.1896	0.0700	0.1689	0.0260	0.8139	7.4886	0.0743	0.1917	0.0229	0.1341	0.0402	0.8369
	$\mathcal{P}_t^{(mv)}$	12.2374	0.0983	0.1633	0.0951	0.1873	0.0349	**0.7524**	7.3059	0.0670	0.2420	0.0532	0.2124	0.0416	**0.7755**
	$\mathcal{P}_t^{(*m)}$	12.3288	0.0494	0.1892	0.0575	0.1740	0.0184	**0.7832**	7.3973	0.0206	0.1874	0.0247	0.1949	0.0822	0.8062
FAHMM		11.6895	0.0451	0.1325	0.0510	0.1926	0.0815	0.5682	6.7580	0.0574	0.1799	0.0401	0.1511	0.0310	0.5912
		11.3242	0.0557	0.1547	0.0527	0.1994	0.0471	**0.4453**	6.6667	0.0423	0.1638	0.0779	0.1717	0.0949	0.5605
		11.2328	0.0611	0.2090	0.0284	0.1709	0.0684	**0.4146**	6.5753	0.0877	0.2197	0.0358	0.2227	0.0311	**0.5298**
		10.9589	0.0160	0.1852	0.0406	0.2378	0.0420	**0.3625**	6.4840	0.0261	0.1592	0.0584	0.1289	0.0410	**0.4991**
SSSM		10.4109	0.4475	0.3667	0.5615	0.5419	0.4091	**0.2381**	5.5708	0.3812	0.5476	0.5888	0.5619	0.4094	**0.2920**
		10.6849	0.4157	0.3392	0.5180	0.4891	0.3679	**0.3303**	5.7534	0.2309	0.4193	0.4665	0.4276	0.2836	**0.3441**
		10.5936	0.4326	0.3556	0.5417	0.5250	0.3822	**0.2842**	5.6621	0.2870	0.5074	0.5361	0.5169	0.3440	**0.3228**
		10.2283	0.5200	0.4583	0.6322	0.6091	0.4960	**0.1768**	5.4794	0.4386	0.6240	0.6595	0.6506	0.4832	**0.2612**
MFHMM		10.5936	0.0825	0.2024	0.0980	0.3674	0.0417	**0.2996**	5.9361	0.0687	0.3876	0.0569	0.3862	0.0319	**0.4148**
		10.5022	0.0316	0.2763	0.0405	0.4139	0.0532	**0.2689**	5.8445	0.0739	0.4478	0.0623	0.4582	0.0816	**0.3840**
		10.7763	0.0391	0.2060	0.0866	0.3255	0.0738	0.3611	6.0274	0.0152	0.4912	0.0366	0.4614	0.0224	0.4455
		10.3196	0.0958	0.2649	0.0516	0.3769	0.0351	**0.2075**	5.7534	0.0798	0.4605	0.0187	0.4341	0.0733	**0.3534**
CHMFA		10.1370	0.6174	0.4980	0.7194	0.6537	0.5937	**0.1461**	5.2055	0.5251	0.6571	0.7814	0.7546	0.5374	**0.1691**
		10.0457	0.5893	0.4396	0.6751	0.6453	0.5071	**0.1154**	5.1142	0.4238	0.5520	0.5790	0.6231	0.4782	**0.1384**
		10.0457	0.5397	0.4669	0.6658	0.6571	0.5650	**0.1234**	5.0230	0.3918	0.6536	0.6739	0.7045	0.4937	**0.1077**
		10.2283	0.6269	0.6503	0.7682	0.7945	0.6753	**0.1622**	5.2968	0.6273	0.7441	0.7725	0.8116	0.6220	**0.1998**

Table 6. Results of the backtesting experiments using different models and different allocation strategies for the confidence levels 98% and 99% on the period October 01, 2019-September 30, 2022.

		VaR 2%							VaR 1%						
Model	$\mathcal{P}_t$	% Hits	UC	IND	CC	DQ	VQ	AQL	% Hits	UC	IND	CC	DQ	VQ	AQL
CHFM	$\mathcal{P}_t^{(m)}$	4.8401	0.0069	0.0197	0.0316	0.0365	0.0371	0.9551	3.9269	0.0361	0.0411	0.0281	0.0141	0.0226	0.9843
	$\mathcal{P}_t^{(me)}$	4.7488	0.0082	0.0207	0.0388	0.0392	0.0403	0.9244	3.8356	0.0372	0.0422	0.0309	0.0164	0.0245	0.9536
	$\mathcal{P}_t^{(mv)}$	4.5662	0.0087	0.0217	0.0393	0.0400	0.0410	0.8630	3.6530	0.0389	0.0446	0.0311	0.0188	0.0272	0.8922
	$\mathcal{P}_t^{(*m)}$	4.6575	0.0078	0.0204	0.0385	0.0388	0.0399	0.8937	3.7443	0.0368	0.0419	0.0304	0.0157	0.0240	0.9229
FAHMM		3.9269	0.0062	0.0190	0.0310	0.0360	0.0364	0.6480	3.0137	0.0357	0.0405	0.0274	0.0136	0.0222	0.6772
		3.8356	0.0106	0.0227	0.0350	0.0438	0.0441	0.6173	2.9224	0.0379	0.0481	0.0324	0.0175	0.0243	0.6465
		3.7443	0.0158	0.0282	0.0407	0.0509	0.0482	**0.5866**	2.8310	0.0424	0.0558	0.0387	0.0228	0.0307	0.6158
		3.6529	0.0236	0.0328	0.0450	0.0587	0.0523	**0.5559**	2.7397	0.0502	0.0586	0.0444	0.0275	0.0368	0.5851
SSSM		2.4657	0.2674	0.1013	0.3829	0.3246	0.2066	**0.2566**	1.6438	0.0276	0.3360	0.0251	0.2698	0.0516	**0.2165**
		2.5570	0.2395	0.1780	0.2244	0.2263	0.1779	**0.2873**	1.7352	0.0650	0.2224	0.0237	0.2749	0.0950	**0.2372**
		2.6484	0.1654	0.1206	0.3201	0.2374	0.0925	**0.3181**	1.8264	0.0723	0.2476	0.0541	0.2633	0.0331	0.2380
		2.2831	0.3002	0.1641	0.4329	0.4197	0.3275	**0.1952**	1.3698	0.0519	0.4025	0.0629	0.4916	0.0482	**0.2244**
MFHMM		3.5616	0.0394	0.0307	0.0598	0.1861	0.0723	**0.5251**	2.6484	0.0493	0.1716	0.0414	0.2303	0.0529	**0.2446**
		3.4703	0.0628	0.1116	0.0293	0.1965	0.0384	0.4946	2.5571	0.0507	0.2230	0.0385	0.2716	0.0425	**0.2449**
		3.3790	0.0076	0.0029	0.0445	0.1090	0.0405	0.4638	2.4657	0.0438	0.2633	0.0326	0.3012	0.0158	0.3160
		3.2877	0.0983	0.0397	0.0718	0.1813	0.0031	**0.4330**	2.3744	0.0287	0.3050	0.0448	0.2782	0.0171	0.2458
CHMFA		2.1917	0.4262	0.3067	0.5623	0.4643	0.3961	**0.1645**	1.2785	0.3858	0.4909	0.6670	0.5723	0.4218	**0.1937**
		2.0091	0.4624	0.3401	0.4850	0.4462	0.3766	**0.1306**	1.0958	0.2504	0.3983	0.4147	0.4629	0.3590	**0.1322**
		2.2831	0.3872	0.2718	0.5495	0.5184	0.4346	**0.1763**	1.3698	0.2333	0.4792	0.5069	0.5578	0.3846	**0.2139**
		2.1004	0.4379	0.4917	0.5806	0.6745	0.5415	**0.1338**	1.1872	0.4558	0.6271	0.6350	0.6559	0.4791	**0.1630**

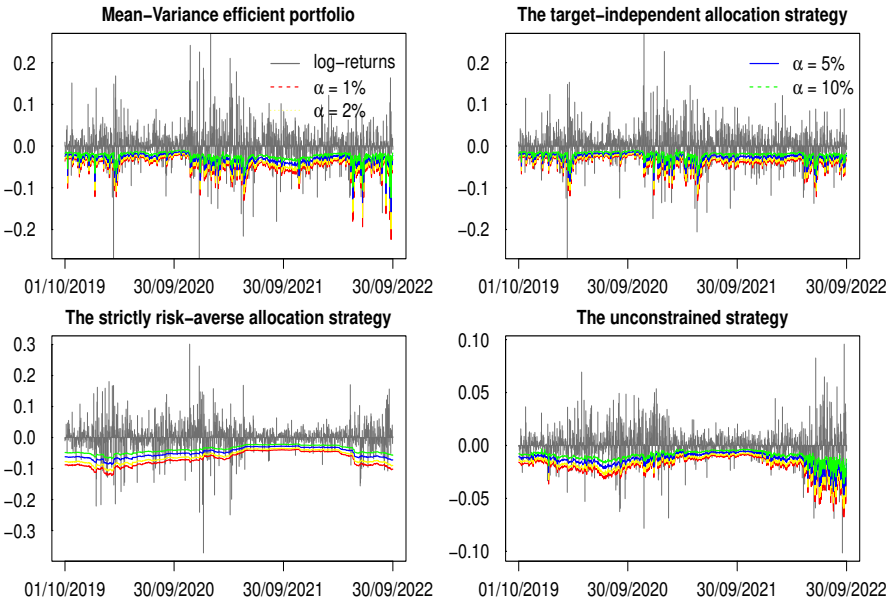

Figure 7. Value-at-Risk for the different allocation strategies for the period from 01-10-2019 to 30-09-2021.

into account simultaneously the level and the regime switches in volatility. Accordingly, the risk manager should account for volatility jumps and sudden shifts the time-varying co-movements among the different heterogeneous crypto asset returns in order to better assess portfolio risks. In this situation, our composite hidden Markov factor analysis model may be used to calibrate factor rotation strategies and to visualize how the co-movement structure has evolved over time. In this context, a Monte Carlo simulation-based CHMFA approach should be more appropriate to build the multivariate loss distribution for the different dynamic allocation strategies.

Finally, all the backtesting results about the ES are given in Table 7. To verify whether the ES is correctly estimated, we used for the different allocation strategies the McNeil and Frey (2000) (McF) test as well as the Bayer and Dimitriadis (2018) (BD) and Nolde and Ziegel (2017) (NZ) tests. For each model, if the p-value is greater than the significance level, then the null hypothesis must not be rejected and the predicted ES does not significantly differ from the expected one. In this case, the McF tests whether the mean of the exceedance residuals is zero. The NZ and BD tests verify whether the predicted ES is accurately determined relative to a realized return series.

We can see from this table that for the coverage rates 10% and 5%, the corresponding p-values of our CHMFA model are largely greater than 0.05, regardless the allocation strategy used. Moreover, when the SSSM and MFHMM are used all the p-values are also greater than 0.05, which imply that these models give an adequate overall fit to the data and an accurate prediction for the ES. For the different allocation strategies and the ES 1%, only the p-values of the optimal CHMFA model are greater that 0.05. For the coverage rate 2%, the best SSSM gives also accurate predictions for the mean-variance efficient portfolio, the target-independent allocation strategy and the strictly risk-averse strategy. All these results confirm that the use of the Monte Carlo simulation-based CHMFA procedure described in Section 3.2 along with the different dynamic allocation strategies yields good ES estimates.

Note finally that McF and NF can be also used to verify the accuracy of the VaR estimation results given in tables 5 and 6. According to these results, we conclude that our CHMFA-based approach performed clearly better than the other competing models for the different allocation strategies and the different confidence levels.

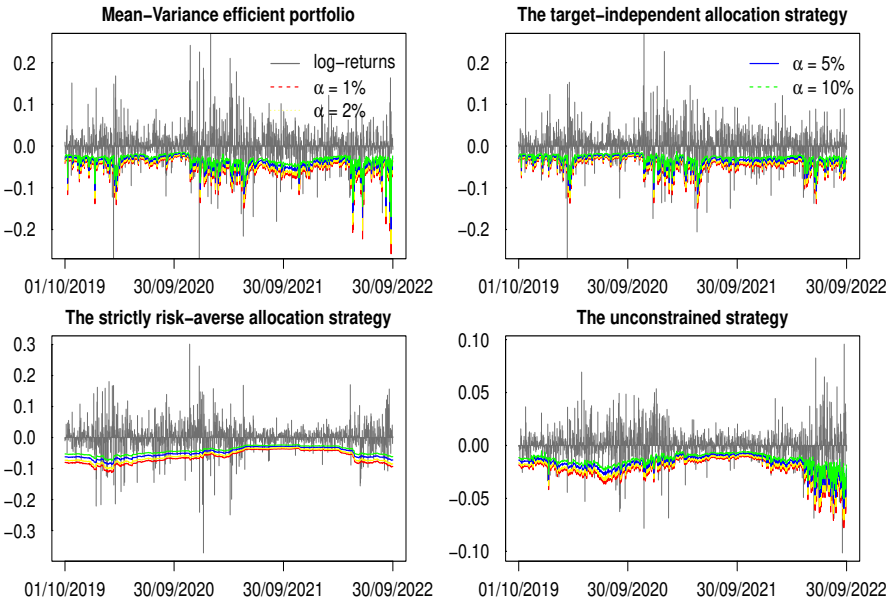

Figure 8. Expected Shortfall for the different allocation strategies for the period from 01-10-2019 to 30-09-2021.

5. Conclusion

This article has proposed a Markov-switching multivariate framework for modeling the latent volatility dynamics as well as the comovements within cryptocurrency markets and the time-varying correlations between cryptocurrencies.

Our model is enough general and flexible and can be extended to contain multiple hidden states and a mixture of conditionally heteroskedastic and standard latent factors, thanks to the employed Variational-EM algorithm. It also shows a good forecasting accuracy, when applied to crypto asset selection using different allocation strategies in a rolling window exercise. The forecast accuracy measures and the encompassing tests show that the composite hidden Markov factor analysis model gives more accurate predictions than those obtained by typical benchmarks. Here, we can argue that the correlations between the cryptocurrency returns expressed by the common latent factors seem to be a valuable information for forecasting. In terms of cumulative financial returns, our framework provides also the best performing portfolio for the different dynamic allocation strategies.

Furthermore, using the composite hidden Markov factor analysis approach for the log-returns of the Bitcoin, Litecoin, DASH, Ethereum, Ripple, and the Stellar currencies, over the period 01/10/2018-31/09/2022, our results show a significant improve in the forecasting performance of the Value-at-Risk (VaR) and the Expected Shortfall (ES) of the optimal crypto-portfolio for the different allocation strategies. This confirms that our model is more suitable for the risk assessment during periods of high volatility and increasing uncertainty, which often coincides with increased speculation in the market. In such periods, non-switching models, are substantially inferior in VaR and ES predictions suggesting that a comparison of predicted losses could serve as an easy, empirical pre-screening device to detect such speculative bubbles.

Note finally that our model can be generalized to account for the time variability in the idiosyncratic risk and to allow for non-homogeneous transition probabilities that depend on the time of day. These extensions would also allow to further flexibility in the crypto asset allocation process and market risk management.

Table 7. Backtesting results of the ES on the period October 01, 2019-September 30, 2022.

		ES 10%			ES 5%			ES 2%			ES 1%		
Model	$\mathcal{P}_t$	McF	NF	BD	McF	NF	BD	McF	NF	BD	McF	NF	BD
CHFM	$\mathcal{P}_t^{(m)}$	0.0245	0.0402	0.0276	0.0378	0.0314	0.0309	0.0407	0.0394	0.0232	0.0242	0.0377	0.0016
	$\mathcal{P}_t^{(me)}$	0.0226	0.0201	0.0172	0.0261	0.0379	0.0347	0.0153	0.0083	0.0307	0.0356	0.0421	0.0024
	$\mathcal{P}_t^{(mv)}$	0.0154	0.0386	0.0223	0.0352	0.0212	0.0260	0.0294	0.0346	0.0171	0.0137	0.0134	0.0381
	$\mathcal{P}_t^{(*m)}$	0.0237	0.0204	0.0322	0.0341	0.0201	0.0366	0.0229	0.0062	0.0275	0.0269	0.0364	0.0144
FAHMM		0.0382	0.0354	0.0334	0.0443	0.0429	0.0309	0.0416	0.0377	0.0435	0.0395	0.0330	0.0366
		0.0347	0.0386	0.0378	0.0336	0.0374	0.0320	0.0354	0.0313	0.0405	0.0422	0.0381	0.0412
		0.0458	0.0353	0.0322	0.0365	0.0455	0.0443	0.0388	0.0307	0.0331	0.0429	0.0377	0.0365
		0.0364	0.0402	0.0443	0.0458	0.0357	0.0445	0.0339	0.0399	0.0445	0.0388	0.0362	0.0405
SSSM		0.5728	0.4321	0.5537	0.4706	0.2536	0.4599	0.1217	0.0932	0.1032	0.0319	0.0354	0.0361
		0.4149	0.6154	0.4139	0.3718	0.6444	0.3631	0.0928	0.0643	0.0859	0.0403	0.0432	0.0470
		0.3891	0.3305	0.4185	0.3812	0.3002	0.4266	0.1486	0.1698	0.1422	0.0484	0.0203	0.0230
		0.6416	0.4030	0.4081	0.5174	0.3956	0.3174	0.0255	0.0413	0.0423	0.0343	0.0281	0.0391
MFHMM		0.1168	0.2029	0.4348	0.3842	0.1384	0.0848	0.0462	0.0481	0.0233	0.0360	0.0168	0.0218
		0.3576	0.2964	0.1057	0.1693	0.2317	0.1243	0.0369	0.0136	0.0431	0.0357	0.0417	0.0367
		0.2685	0.3451	0.4400	0.3037	0.4147	0.2123	0.0386	0.0388	0.0209	0.0490	0.0235	0.0431
		0.1828	0.2271	0.1184	0.2499	0.1280	0.3485	0.0129	0.0419	0.0263	0.0103	0.0425	0.0354
CHMFA		0.7755	0.5403	0.9469	0.5951	0.6791	0.6827	0.8162	0.5350	0.7897	0.5282	0.8171	0.6881
		0.7317	0.6406	0.8444	0.8105	0.6553	0.5984	0.6308	0.7656	0.9075	0.6985	0.5183	0.9120
		0.5236	0.7227	0.7699	0.6112	0.7062	0.6445	0.6170	0.9345	0.6511	0.7156	0.9427	0.6323
		0.5244	0.7001	0.5124	0.6848	0.6771	0.6678	0.8566	0.5911	0.8480	0.5334	0.5275	0.5017

REFERENCES

1. Abbara, O., and Zevallos, M. (2018). Modeling and Forecasting Intraday VaR of an Exchange Rate Portfolio. *Journal of Forecasting*, 37 (7), pp. 729-738.
2. Alizadeh, S., Brandt, M. W., and Diebold, F. X. (2002). Range-Based Estimation of Stochastic Volatility Models. *The Journal of Finance*, 57 (3), pp. 1047-1091.
3. Bayer, S., and Dimitriadis, T., (2018). Regression Based Expected Shortfall Backtesting. arXiv preprint. [online] https://arxiv.org/abs/1801.04112
4. Bera, A. K., and Jarque, C. M. (1982). Model specification tests: A simultaneous approach. *Journal of Econometrics*, 20 (1), pp. 59-82.
5. Charles, A., and Darné, O. (2019). Volatility Estimation for Cryptocurrencies: Further Evidence with Jumps and Structural Breaks. *Economics Bulletin*, 39 (2), pp. 954-968.
6. Chen, X., and Yin, X. (2019). Solve Nonlinear Optimization with Nonlinear Constraints, Version 0.6. [online] https://cran.r-project.org/web/packages/NlcOptim/NlcOptim.pdf
7. Christoffersen, P. F., (1998). Evaluating Interval Forecasts. *International Economic Review*, 29 (4), pp. 841-862.
8. Dempster, A., Laird, N., and Rubin, D. (1977). Maximum Likelihood from incomplete data via the EM algorithm. *Journal of Royal Statistical Society Series B*, 39 (1), pp. 1-38.
9. Elendner, H., Trimborn, S., Ong, B., and Lee, T. M. (2017). The Cross-Section of Cryptocurrencies as Financial Assets: Investing in Cryptocurrencies Beyond Bitcoin. In *Handbook of Blockchain, Digital Finance, and Inclusion*, Volume 1: Cryptocurrency, FinTech, InsurTech, and Regulation, Elsevier, pp. 145-173.
10. Engle, R. F., and Manganelli, S., (2004). CAViaR: Conditional Autoregressive Value at Risk by Regression Quantiles. *Journal of Business & Economic Statistics*, 22 (4), pp. 367-381.
11. Gaglianone, W. P., Lima, L. R., Linton, O., and Smith, D. R. (2011). Evaluating Value-at-Risk Models via Quantile Regression. *Journal of Business & Economic Statistics*, 29 (1), pp. 150-160.
12. Gkillas, K. and Katsiampa, P. (2018). An application of extreme value theory to cryptocurrencies. *Economics Letters*, 164 (C), pp. 109-111.
13. Gonzalez-Rivera, G., Lee, T. H., and Mishra, S. (2004). Forecasting Volatility: A Reality Check Based on Option pricing, Utility function, Value-at-Risk, and Predictive Likelihood. *International Journal of Forecasting*, 20 (4), pp. 629-645.
14. Hansen, P. R., Lunde, A., and Nason, J. M. (2011). The Model Confidence Set. *Econometrica*, 79 (2), pp. 453-497.
15. Harvey, D. I., Leybourne, S., and Newbold, P. (1998). Tests for forecast encompassing. *Journal of Business and Economic Statistics*, 16 (2), pp. 254-259.
16. Harvey, A., Ruiz, E., and Sentana, E. (1992). Unobserved component time series models with ARCH disturbances. *Journal of Econometrics*. 52 (1-2), pp. 129-157.
17. Kupiec, P. H. (1995). Techniques for Verifying the Accuracy of Risk Measurement Models. *The Journal of Derivatives*, 3 (2), pp. 73-84.
18. Levy, B. P., and Lopes, H. F. (2021a). Dynamic Ordering Learning in Multivariate Forecasting. arXiv preprint. [online] https://arxiv.org/pdf/2101.04164.pdf
19. Levy, B. P., and Lopes, H. F. (2021b). Dynamic Portfolio Allocation in High Dimensions using Sparse Risk Factors. arXiv preprint. [online] https://arxiv.org/pdf/2105.06584.pdf
20. Liu, W., Semeyutin, A., Lau, C. K. M., and Gozgor, G. (2020). Forecasting Value-at-Risk of Cryptocurrencies with RiskMetrics type models. *Research in International Business and Finance*, 54, 101259.
21. Ljung, G., and Box, G. (1978). On a Measure of Lack of Fit in Time Series Models. *Biometrika*, 65 (2), pp. 297-303.
22. Maciel, L. (2020). Cryptocurrencies value-at-risk and expected shortfall: Do regime-switching volatility models improve forecasting? *International Journal of Finance & Economics*, pp. 1-16.
23. Markowitz, H. M. (1952). Portfolio Selection. *The Journal of Finance*, 7 (1), pp. 77-91.
24. McNeil, A. J., and Frey, R. (2000). Estimation of Tail-related Risk Measures for Heteroscedastic Financial Time Series: An Extreme Value Approach. *Journal of Empirical Finance*, 7 (3–4), pp. 271-300.
25. Nolde, N., and Ziegel, J. F. (2017). Elicitability and Backtesting: Perspectives for Banking Regulation. *The Annals of Applied Statistics*, 11 (4), pp. 1833-1874.
26. Petukhina, A., Trimborn, S., Hardle, W. K., and Elendner, H. (2021). Investing with cryptocurrencies - evaluating their potential for portfolio allocation strategies. *Quantitative Finance*, 21 (11), pp. 1825-1853.
27. Saidane, M. (2023). Sequential Forecasting Strategies for Crypto Portfolio Allocation: A Dynamic Latent Factor Analysis Approach. *Journal of Administrative and Economic Sciences*, 16 (2), pp. 61-84.
28. Saidane, M. (2022a). A New Viterbi-Based Decoding Strategy for Market Risk Tracking: an Application to the Tunisian Foreign Debt Portfolio during 2010-2012. *Statistika: Statistics and Economy Journal*, 102 (4), pp. 454-470.
29. Saidane, M. (2022b). Switching latent factor value-at-risk models for conditionally heteroskedastic portfolios: A comparative approach. *Communications in Statistics: Case Studies, Data Analysis and Applications*, 8 (2), pp. 282-307.
30. Saidane, M. (2019). Forecasting Portfolio-Value-at-Risk with Mixed Factorial Hidden Markov Models. *Croatian Operational Research Review*, 10 (2), pp. 241-255.
31. Saidane, M. (2017). A Monte-Carlo-based Latent Factor Modeling Approach with Time-Varying Volatility for Value-at-Risk Estimation: Case of the Tunisian Foreign Exchange Market. *Industrial Engineering & Management Systems*, 16 (3), pp. 400-414.
32. Saidane, M., Lavergne, C. (2011). Can the GQARCH Latent Factor Model Improve the Prediction Performance of Multivariate Financial Time Series? *American Journal of Mathematical and Management Sciences*, 31 (1,2), pp. 73-116.
33. Saidane, M., and Lavergne, C. (2009). Optimal Prediction with Conditionally Heteroskedastic Factor Analysed Hidden Markov Models. *Computational Economics*, 34 (4), pp. 323-364.
34. Saidane, M., and Lavergne, C. (2008). An EM-Based Viterbi Approximation Algorithm for Mixed-State Latent Factor Models. *Communications in Statistics - Theory and Methods*, 37 (17), pp. 2795-2814.

35. Saidane, M., and Lavergne, C. (2007a). A structured variational learning approach for switching latent factor models. *Advances in Statistical Analysis - AStA*, 91 (3), pp 245-268.
36. Saidane, M., and Lavergne, C. (2007b). Conditionally heteroscedastic factorial HMMs for time series in finance. *Applied Stochastic Models in Business and Industry*, 23 (6), pp. 503-529.
37. Saidane, M., and Lavergne, C. (2006). On factorial HMMs for time series in finance. *The Kyoto Economic Review*, 75 (1), pp. 23-50.
38. Schwarz, G. (1978). Estimating the dimension of a model. *Annals of Statistics*, 6 (2), pp. 461-464.
39. Takeda, A. and Sugiyama, M. (2008). N-Support Vector Machine As Conditional Value-At- Risk Minimization. *Proceedings of the 25-th International Conference on Machine Learning*, pp. 1056-1063.
40. Troster, V., Tiwari, V, Shahbaz, M., and Macedo, D. N. (2019). Bitcoin Returns and Risk: A General GARCH and GAS Analysis. *Finance Research Letters*, 30 (6), pp. 187-193.
41. Trucios, C. (2019). Forecasting Bitcoin Risk Measures: A Robust Approach. *International Journal of Forecasting*, 35 (3), pp. 836-847.
42. Trucios, C., Tiwari, A. K., and Alqahtani, F. (2020). Value-at-risk and expected shortfall in cryptocurrencies' portfolio: A vine copula-based approach. *Applied Economics*, 52 (24), pp. 2580-2593.
43. Yu, W., Yang, K., Wei, Y., and Lei, L. (2018). Measuring Value-at-Risk and Expected Shortfall of Crude Oil Portfolio Using Extreme Value Theory and Vine Copula. *Physica A: Statistical Mechanics and Its Applications*, 490 (C), pp.1423-1433.